BIOMOLECULES & THERAPEUTICS

**Original Article**
*Biomol Ther 29(5), 483-491 (2021)*

# Matrix Metalloproteinase-8 Inhibitor Ameliorates Inflammatory Responses and Behavioral Deficits in LRRK2 G2019S Parkinson's Disease Model Mice

**Taewoo Kim[1,†], Jeha Jeon[1,†], Jin-Sun Park[2], Yeongwon Park[1], Jooeui Kim[1], Haneul Noh[1], Hee-Sun Kim[2,*] and Hyemyung Seo[1,*]**

*[1]Department of Molecular & Life Sciences, Center for Bionano Intelligence Education and Research, Hanyang University, Ansan 15588,*
*[2]Department of Molecular Medicine and Medical Research Institute, School of Medicine, Ewha Womans University, Seoul 07804, Republic of Korea*

## Abstract

Parkinson's disease (PD) is a neurodegenerative disorder that involves the loss of dopaminergic neurons in the substantia nigra (SN). Matrix metalloproteinases-8 (MMP-8), neutrophil collagenase, is a functional player in the progressive pathology of various inflammatory disorders. In this study, we administered an MMP-8 inhibitor (MMP-8i) in Leucine-rich repeat kinase 2 (LRRK2) G2019S transgenic mice, to determine the effects of MMP-8i on PD pathology. We observed a significant increase of ionized calcium-binding adapter molecule 1 (Iba1)-positive activated microglia in the striatum of LRRK2 G2019S mice compared to normal control mice, indicating enhanced neuro-inflammatory responses. The increased number of Iba1-positive activated microglia in LRRK2 G2019S PD mice was down-regulated by systemic administration of MMP-8i. Interestingly, this LRRK2 G2019S PD mice showed significantly reduced size of cell body area of tyrosine hydroxylase (TH) positive neurons in SN region and MMP-8i significantly recovered cellular atrophy shown in PD model indicating distinct neuro-protective effects of MMP-8i. Furthermore, MMP-8i administration markedly improved behavioral abnormalities of motor balancing coordination in rota-rod test in LRRK2 G2019S mice. These data suggest that MMP-8i attenuates the pathological symptoms of PD through anti-inflammatory processes.

**Key Words:** Parkinson's disease (PD), Matrix metalloproteinase-8 (MMP-8), Neuro-inflammation, Neuroprotection

## INTRODUCTION

Parkinson's disease (PD) is a neurodegenerative disorder characterized by the loss of dopaminergic neurons in the substantia nigra (SN) and alpha-synuclein deposits in various brain regions (Hirsch *et al*., 1988, 2003). The degeneration of dopaminergic neurons in the SN results in reduced striatal dopamine content and motor dysfunction, including rigidity and tremor (Braak *et al*., 2003). A number of studies have demonstrated that activated microglia produce and release various proinflammatory markers and have suggested strong correlations between microglial activation and dopaminergic degeneration as one of the critical pathogenic factors for PD (Liu, 2006; Frank *et al*., 2007; Ghosh *et al*., 2007; Lyons *et al*., 2007; Moon *et al*., 2009; Ros-Bernal *et al*., 2011).

Matrix metalloproteinases (MMPs) are zinc-dependent endopeptidases that degrade extracellular matrix (ECM). MMPs are involved in normal embryogenesis, tissue morphogenesis, and tumor cell development (Rooprai *et al*., 2000; Abdullah Thani *et al*., 2012). MMPs are patho-physiological regulators of PD. Abnormal regulation of various MMP functions has been reported in PD models and patients. For example, MMP-2 levels were reduced in the substantia nigras of post-mortem brains of PD patients (Lorenzl *et al*., 2002). MMP-9 was elevated in MPTP-induced parkinsonism in mice, and an MMP inhibitor suppresses dopaminergic cell death (Lorenzl *et al*., 2004). MMP-3 knockout mice showed attenuated neuronal cell death and dopamine depletion in an MPTP-induced

**Open Access** **https://doi.org/10.4062/biomolther.2020.181**



**Received** Oct 15, 2020 **Revised** Mar 15, 2021 **Accepted** Apr 28, 2021
**Published Online** May 28, 2021

***Corresponding Authors**
E-mail: hseo@hanyang.ac.kr (Seo H), hskimp@ewha.ac.kr (Kim HS)
Tel: +82-31-400-5511 (Seo H), +82-2-6986-6270 (Kim HS)
Fax: +82-31-419-1760 (Seo H), +82-2-6986-7014 (Kim HS)
[†]The first two authors contributed equally to this work.

PD model, suggesting a role for MMP-3 in the pathogenesis of PD (Kim *et al*., 2007). Papaverine (PAP) inhibited dopaminergic neuronal cell death and α-synuclein aggregation by repressing expression level of MMP-3 and neuroinflammation in MPTP PD model mice (Leem *et al*., 2020). MMP-1 and -3 induced the cleavage of α-synuclein, increasing α-synuclein aggregation and neurotoxicity, which is associated with PD pathogenesis (Sung *et al*., 2005; Levin *et al*., 2009). Previously, our group reported that MMP-3, MMP-8, and MMP-9 play an important role in α-synuclein-induced microglial activation by activating protease-activated receptor-1 (Lee *et al*., 2010). Moreover, inhibition of MMP-3, -8, or -9 significantly suppressed proinflammatory cytokine expression and upstream signaling pathways induced by α-synuclein (Lee *et al*., 2010).

MMP-8 is a neutrophil collagenase that is associated with various inflammatory disorders, such as atherosclerosis, periodontitis, pulmonary disease, diabetes, and cancer (van der Zijl *et al*., 2010; Sorsa *et al*., 2011; Väyrynen *et al*., 2012). The absence of MMP-8 induced an increase in tumor susceptibility and an anti-fibrotic effect with an increase in IL-10 (Balbin *et al*., 2003; Gueders *et al*., 2005; Van Lint *et al*., 2005; Gutierrez-Fernandez *et al*., 2007; Garcia-Prieto *et al*., 2010). Recent studies have examined MMP-8 in various neuroinflammatory disorders. In bacterial meningitis, MMP-8 degrades occludin, one of the blood-brain barrier (BBB) components, and induces neuroinflammation (Schubert-Unkmeir *et al*., 2010). In experimental autoimmune encephalomyelitis (EAE), an animal model of human multiple sclerosis, MMP-8 modulates Th1/Th2 polarization, which results in inflammation and demyelination (Folgueras *et al*., 2008). Administration of an MMP-8 inhibitor or MMP-8 knockout mice led to attenuation of BBB breakdown and EAE progression. MMP-8 inhibitor significantly reduced TNF-α, IL-6, and iNOS expression levels and increased tight junction proteins expression in rat model of spinal cord injury (SCI) (Kumar *et al*., 2018). Our group recently reported on the proinflammatory role of MMP-8 in microglial activation (Lee *et al*., 2014). In LPS-stimulated microglia, MMP-8 is involved in TNF-α processing; therefore, specific inhibition of MMP-8 strongly suppressed TNF-α secretion. In addition, administration of an MMP-8 inhibitor or MMP-8 shRNA reduced inflammatory responses in mouse brains with systemic inflammation and cerebral ischemia (Lee *et al*., 2014; Han *et al*., 2016). Moreover, MMP-8 inhibitor enhanced antioxidant effect by modulating Nrf2/ARE signaling pathway in lipoteichoic acid-stimulated rat primary astrocytes (Lee *et al*., 2018). Furthermore, inhibition of MMP-8 significantly reduced infarct volume and neuronal cell death in the ischemic mouse brain (Han *et al*., 2016).

Although a number of previous studies have found that MMP-8 plays an important role in neuronal cell death and neuroinflammation, the role of MMP-8 in *in vivo* PD pathology has not been elucidated. To study the *in vivo* effects of MMP-8 inhibition, we used LRRK2 G2019S mice at 20-24 months of age. LRRK2 is associated with autosomal dominant and late-onset PD and LRRK2 G2019S mutations increased kinase activity and decreased cellular viability (Smith *et al*., 2006). LRRK2 G2019S mutant mice showed alpha-synuclein inclusion bodies and impairment of chaperone-mediated autophagy (Orenstein *et al*., 2013). The MMP-8 inhibitor (MMP-8i) used in this study is known to be MMP-8 specific because it reduced mortality and inflammatory markers in a murine model of sepsis and because it reproduced the MMP-8 -/- phenotype (Solan *et al*., 2012). This MMP-8i markedly inhibited LPS-induced MMP-8 activity without altering MMP-3 or MMP-9 activities in LPS-stimulated BV2 microglia (Lee *et al*., 2014). In the present study, we examined the effects of MMP-8i on the PD pathology of LRRK2 G2019S mice to evaluate neuroinflammation, cellular oxidative stress, mitochondrial activities, neuronal viability, cellular morphology, and motor balancing coordination behaviors.

## MATERIALS AND METHODS

### Experimental animals and MMP-8 inhibitor administration

LRRK2 G2019S mutant mice (FVB/N-Tg 1Cjli/J, Jackson Laboratory, Bar Harbor, ME, USA) were purchased and housed under a 12 h light-dark cycle with free access to food. All experiments were performed according to the guidelines of the Institutional Animal Care and Use Committee (IACUC) of Hanyang University (Seoul, Korea) (HY-IACUC-12-018). We used MMP-8 inhibitor (MMP-8i) which showed specific and efficient inhibition of MMP-8 in previous studies (Solan *et al*., 2012; Lee *et al*., 2014). We injected MMP-8i (Calbiochem, San Diego, CA, USA; 5 mg/kg, i.p., once per day for 4 days) or 1% dimethyl sulfoxide (DMSO) as a vehicle into male LRRK2 G2019S mice.

In this study, 17 male mutant mice (vehicle injection: MMP-8i injection=9:8) and 16 male littermate control mice (vehicle injection: MMP-8i injection=9:7) at age of 20-24 months were used for behavioral and biochemical analysis. On the last day of injection (4$^{th}$ day), all mice were tested in the rota-rod and open field tests and sacrificed 8 h after the final injection.

### Rota-rod test

We tested all experimental mice with the rota-rod and open field tests to determine motor coordination and locomotor activities. The rota-rod test was performed first in four consecutive trials (5 rpm, for a period of 60 s) as previously described (Seo *et al*., 2008), and the latency to fall from the rotating rod (Panlab, Barcelona, Spain) was video-recorded and statistically analyzed using SPSS program (IBM, Armonk, NY, USA).

### Open field test

For the open field test, mice were placed in the center of a clear acrylic box (27.5×27.5 cm$^2$) with a black line divided into 25 squares (5.5×5.5 cm$^2$ each). Mouse movements were counted and recorded for three trials (4 min per trial) with no interval. The total number of rearing and wall-rearing were counted to detect motor ability. The time spent in the center square area was also counted to detect anxiety-like behavior. All the motor activities were video-recorded and statistically analyzed using SPSS program (IBM).

### Immunohistochemical analysis

For immunohistochemical analysis, mice were perfused with phosphate-buffered saline (PBS) and then 4% paraformaldehyde (PFA), as previously described (Seo *et al*., 2004), and then the brains were removed from the skull, post-fixed in 4% PFA for 3 h, and moved to a 20% sucrose solution for 2 days. Serial sections of the brains were sliced into 30 μm sections on a freezing microtome (Thermo 430, Thermo Fisher Scientific, Walldorf, Germany) and sections were stored in PBS with 0.03% sodium azide at 4°C until use. Brain sections

from experimental groups were incubated in blocking solution with 10% normal goat serum (NGS; Vector Laboratories, Burlingame, CA, USA) for 1 h at RT, and then incubated in various primary antibodies, including polyclonal anti-ionized calcium-binding adapter molecule 1 (Iba1) (1:250; Wako, Osaka, Japan), polyclonal anti-choline acetyltransferase (ChAT) (1:500; Millipore, Bedford, MA, USA), or polyclonal anti-tyrosine hydroxylase (TH) (1:500; Pel-freez, Rogers, AR, USA), for 3 h at RT. They were then incubated with the secondary antibody, HRP-linked anti-rabbit IgG (1:500; Vector Laboratories). After incubation in a diaminobenzidine (DAB) solution (Vector Laboratories), sections were mounted on 0.3% gelatin-coated glass plates and air-dried. After applying a coverslip, we obtained images using a Carl Zeiss microscope (Axio observer, Carl Zeiss, Oberkochen, Germany). The quantification of immuno-reactive cells was carried out following previous studies (Jeon *et al*., 2016). In brief, unbiased stereological methods were applied and blindly confirmed by two different assessors on coded slides. Labelled cells were counted in every twelfth section in one in twelve series, with a total of three sections per animal analyzed. The region of interest was identified at 10×magnification, whereas the cells were quantified at 600×magnification. The areas of the immuno-reactive cells were measured using Image J program (version 1.46r; NIH, Bethesda, MD, USA).

### RNA isolation and quantitative RT-PCR

RNA samples were isolated from the striatum using TRI-reagent (Sigma-Aldrich, St. Louis, MO, USA) following the manufacturer's instruction. The RNA pellet was dried for 10 min and dissolved with DEPC-treated water (Ambion, Austin, TX, USA) and stored at –20°C before use. The Premium express 1st strand cDNA synthesis system (Legene biosciences, San Diego, CA, USA) was used to synthesize the first-strand cDNA from equal amounts (500 ng) of the RNA samples. The cycling reactions were performed in 40 cycles of 95°C for 15 s and 60°C for 1 min. The primer sequences for quantitative RT-PCR is summarized in Table 1. The expression levels of each target gene were normalized by the expression level of beta-actin and presented as group comparison.

**Table 1.** List of primers used for quantitative RT-PCR

| Gene | Primers used |
|---|---|
| CD11b | 5'-GCA GTC ATC TTG AGG AAC CGT GTC-3' (forward) |
| | 5'-GTT GGT ATT GCC ATC AGC GTC C-3' (reverse) |
| CD45 | 5'-CAG AGC ATT CCA CGG GTA TT-3′ (forward) |
| | 5′-GGA CCC TGC ATC TCC ATT TA-3′ (reverse) |
| IL-1β | 5'-CTG GTG TGT GAC GTT CCC ATT A-3' (forward) |
| | 5'-CCG ACA GCA CGA GGC TTT-3' (reverse) |
| IL-6 | 5'-TCC ATC CAG TTG CCT TCT TGG-3' (forward) |
| | 5'-CCA CGA TTT CCC AGA GAA CAT G-3' (reverse) |
| SRA | 5'-GAC GCT TCC AGA ATT TCA GC-3' (forward) |
| | 5'-ATG TCC TCC TGT TGC TTT GC-3' (reverse) |
| TLR2 | 5'-TGC TTT CCT GCT GGA GAT TT-3' (forward) |
| | 5'-TGT AAC GCA ACA GCT TCA GG-3' (reverse) |
| TLR4 | 5'-TGA CAG GAA ACC CTA TCC AGA GTT-3' (forward) |
| | 5'-TCT CCA CAG CCA CCA GAT TCT-3' (reverse) |
| TGF-β | 5'-AAC AAT TCC TGG CGT TAC CTT-3' (forward) |
| | 5'-CTG CCG TAC AAC TCC AGT GA-3' (reverse) |
| iNOS | 5'-TCA GCC AAG CCC TCA CCT AC-3' (forward) |
| | 5'-CCA ATC TCT GCC TAT CCG TCT C (reverse) |
| FcγRII | 5'-GGA AGA AGC TGC CAA AAC TG-3' (forward) |
| | 5'-CCA ATG CCA AGG GAG ACT AA-3' (reverse) |
| TNF-α | 5'-CCC CAA AGG GAT GAG AAG TT-3' (forward) |
| | 5'-CAC TTG GTG GTT TGC TAC GA-3' (reverse) |
| IFN-γ | 5'-GAG GAA CTG GCA AAA GGA TG-3' (forward) |
| | 5'-TGA GCT CAT TGA ATG CTT GG-3' (reverse) |
| β-actin | 5'-GTC CAC ACC CGC CAC CAG TTC G-3' (forward) |
| | 5'-ATG CCG GAG CCG TTG TCG AC-3' (reverse) |
| GAPDH | 5'- ATG AAT ACG GCT ACA GCA -3' (forward) |
| | 5'- GCC CCT CCT GTT ATT ATG G -3' (reverse) |

### Protein sample preparation

For biochemical analysis, the striatum region of the brain was dissected out and the tissue chunks were stored at –80°C before use. Brain tissue chunks of the striatum region were homogenized in 50 mM Tris (pH 8.0), 150 mM NaCl, 5 mM EDTA, 1% Triton X-100 with inhibitors of protease and phosphatase: 10 μg/mL aprotinin, 25 μg/mL leupeptin, 10 μg/mL of pepstatin, 10 μg/mL phenyl-methanesulfonyl fluoride, 50 mM sodium fluoride, and 1 mM sodium orthovanadate (Sigma-Aldrich). The brain lysate was centrifuged at 1,400×g for 5 min at 4°C and the supernatant was collected and centrifuged again at 7,900×g for 15 min. The supernatant after centrifugation was used for the cytoplasmic fraction and the pellet was re-suspended and sonicated for mitochondrial fraction. All protein samples were stored at –80°C until use. Cytoplasmic and mitochondrial fractionation was confirmed with the expression level of mitochondrial protein.

### Immunoblot

Protein samples (20 μg) were used for western blot and slot blot analysis. The following primary antibodies were used: polyclonal anti-LRRK2 (1:2,500; Millipore), monoclonal anti-CD45 (1:2,500; Abcam, Cambridge, MA, USA), polyclonal anti-MMP-8 (1:2,500; Abcam), monoclonal anti-β-actin (1:2,500; Abcam), and monoclonal anti-GAPDH (1:2,500; Millipore). We used horseradish peroxidase (HRP)-linked anti-rabbit (1:2,500; Vector Laboratories, Burlingame, CA, USA) or HRP-linked anti-mouse (1:2,500; Vector Laboratories) IgG antibodies as secondary antibodies. After the incubation with primary and secondary antibodies, the blotted membrane was developed using ECL prime (Merck, Boston, MA, USA). Intensity of each band was quantified using Image J program (version 1.46r; NIH), and normalized to the expression level of β-actin or GAPDH as loading control.

### Determination of glutathione levels (GSH/GSSG)

Cellular levels of glutathione (reduced/oxidized forms, GSH/GSSG) were detected from the cytosolic fraction of the striatum using a GSH/GSSG ratio detection assay kit (Abcam) according to the manufacturer's protocol. Total 10 μg of cytosolic protein samples were loaded for the reaction with the Thiol Green Indicator Reaction Mixture and then incubated at room temperature for 30 min. Enzyme activity was detected at 490/520 nm and normalized to protein amount.

### Determination of ATP levels

ATP levels in the mitochondria fraction were measured by

oxidation of luciferin using the ATP Bioluminescence Assay Kit HS II (Roche, Penzberg, Germany) according to the manufacturer's protocol. The mitochondria samples from the striatum (7.5 μg) or ATP standard solution were loaded into individual wells of a microplate with 50 μL of luciferase reagent. The microplate was immediately read using a microplate reader (562 nm, Synergy H1 Hybrid Multi-Mode Microplate Reader, BioTek, Winooski, VT, USA).

### Determination of mitochondrial complex activities

We determined activities of mitochondrial complexes as previously described (Bouhours-Nouet *et al*., 2005). Briefly, for complex I activity, the mitochondria fraction samples (1 μg) were incubated in 10 mM $KH_2PO_4$ (pH 7.4), with 2 mM KCN, 100 μM decylubiquinone, 1 mg/mL BSA and 200 μM NADH (Sigma-Aldrich). For complex II/III activity, the mitochondria fraction samples (10 μg) were incubated in 40 mM $K_2HPO_4$ (pH 7.4), 20 mM succinate, 50 μM cytochrome c, 0.5 mM EDTA, and 1.5 mM KCN. For complex IV activity, the mitochondria fraction samples (5 μg) were incubated in 10 mM $KH_2PO_4$ (pH 7.4), and 50 μM reduced cytochrome c (reduced using sodium dithionite). The decrease in the absorbance due to the oxidation of substrates was measured at 340 nm for complex I activity, and at 550 nm for complex II/III and complex IV activities. The absorbance for mitochondrial complex activities was detected for 8 h with 3 min intervals at 30°C in a microplate reader (Synergy H1 Hybrid Multi-Mode Microplate Reader, BioTek). Complex activities were normalized to protein amounts and reaction time as nmol/min/mg.

### Statistical analysis of data

All biochemical experiments were triplicated before statistical analyses which were carried out using SPSS (version 21; IBM). Data from RT-PCR, immunoblots, immunohistochemistry, and behavioral tests were analyzed by comparing the MMP-8i injected group with the vehicle injected control group as mean ± SEM using the student's t-test and ANOVA analysis. A *p*-value less than 0.05 was considered statistically significant between groups.

## RESULTS

Previous studies reported that MMP-8 plays an important role in neuroinflammation and neuronal cell death in *in vitro* PD models (Solan *et al*., 2012; Lee *et al*., 2014). In this study, we used MMP-8i, which has been reported for its efficient and specific inhibition of cellular MMP-8 activity (Solan *et al*., 2012; Lee *et al*., 2014) to detect the expression levels of proinflammatory markers, mitochondrial complex activities, and glutathione oxidation/reduction to understand cellular mechanism for morphological alteration, bioenergetics, oxidative stress. In addition, we tested whether MMP-8i can eventually improve locomotor activities in LRRK2 G2019S mice.

### MMP-8i administration reduced the microglial activation

The number of Iba1-positive cells, which represent activated microglia, significantly increased in the striatum of LRRK2 G2019S mice compared to littermate control mice (Fig. 1A). These data indicate enhanced level of neuroinflammation in the LRRK2 G2019S PD model mice used in this study. MMP-8i administration significantly decreased the number of Iba1-positive cells in both LRRK2 G2019S and littermate control mice, suggesting the reduced inflammatory response after MMP-8i administration in PD model mice. Supporting this data, when we determined the expression levels of inflammatory markers including several cytokines (Fig. 1B), we found that significant increase of TGF-β mRNA expression and increasing patterns of the most of inflammatory markers tested as shown in Fig. 1B. However, we could not find the significant decreased of the mRNA expression levels of those inflammatory markers by MMP8i. Interestingly, protein levels of CD45 significantly decreased in striatum of LRRK2 G2019S mice after administration of MMP-8i (Fig. 2A) without significant changes of LRRK2 protein expression.

### MMP-8i administration reduced the expression levels of MMP-8

Previous studies showed that MMP-8i inhibits the activity of MMP-8 and reduces MMP-8 expression levels in a neuroinflammation model (Lee *et al*., 2014). In this study, LRRK2 G2019S mice showed strongly increased MMP-8 protein levels compared to littermate control mice (Fig. 2B). After MMP-8i administration, the mRNA levels of MMP-8 significantly decreased in striatum of LRRK2 G2019S mice. The level of plasma MMP-8 mRNA was significantly higher in LRRK2 G2019S mice compared to littermate control mice, and it significantly decreased after MMP-8i injection (data not shown). This pattern was similar to the protein detection data in the striatum of LRRK2 G2019S mice (Fig. 2B).

### The effect of MMP-8i on oxidative stress and mitochondrial complex activities

To understand the cellular process of neurodegeneration and neuroinflammation after MMP-8i administration, we determined whether MMP-8i changes cellular oxidative stress levels and mitochondrial complex activities. We evaluated glutathione contents to determine the endogenous oxidative stress levels in the striatum of LRRK2 G2019S mice. We detected the level of reduced glutathione (GSH) as a scavenger of reactive oxygen species (ROS), and its ratio with oxidized glutathione (GSSG), GSH/GSSG, as a marker of endogenous oxidative stress (Zitka *et al*., 2012). In our results, LRRK2 G2019S mice did not show significant changes in the GSH/GSSG ratio. In addition, MMP-8i did not significantly change GSH/GSSG ratios in the striatum of both LRRK2 G2019S and littermate control mice (Fig. 3A).

We next measured mitochondrial ATP levels as a parameter of mitochondrial activity to quantify the products of oxidative phosphorylation in mitochondrial energy metabolism. LRRK2 G2019S mice and littermate control mice did not show significant differences in mitochondrial ATP levels. Mitochondrial ATP levels significantly increased in the striatum after MMP-8i administration in littermate control mice (Fig. 3B).

To elucidate how the oxidative phosphorylation to produce ATP gets affected by mitochondrial enzyme activities, we measured mitochondrial complexes, I, II/III, and IV enzyme activities in the striatum of LRRK2 G2019S mice. Although LRRK2 G2019S mice did not show significantly different levels of mitochondrial complex activities, compared to littermate control mice (Fig. 3C), MMP-8i administration did increase complex IV activity in littermate control mice. These data showed similar patterns with the change of ATP levels suggesting potential correlation between mitochondrial complex IV activities and

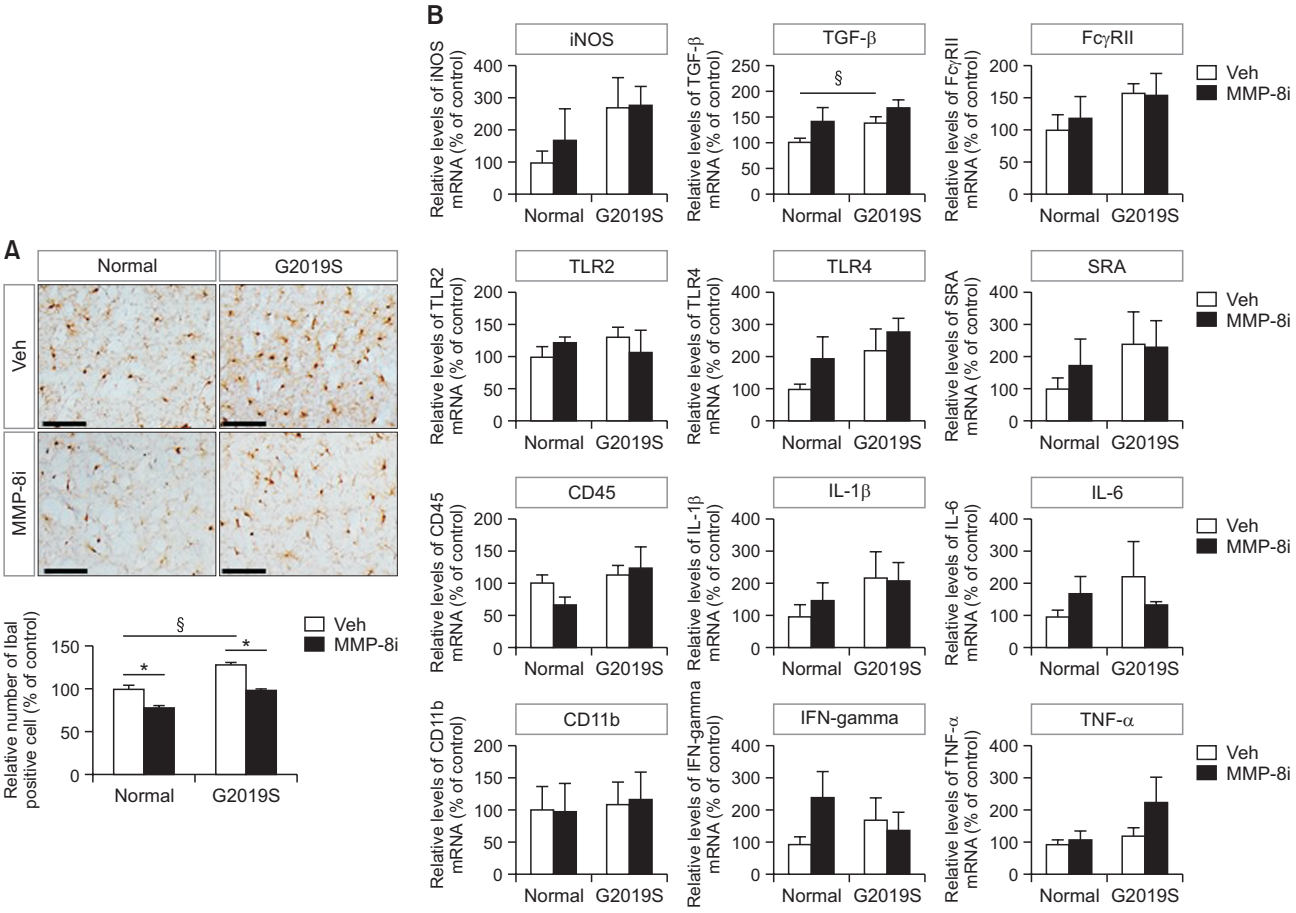


**Fig. 1.** The effects of MMP-8i on proinflammatory markers and microglial activation. (A) The number of Iba1-positive activated microglial cells in the striatum was visualized and quantified by immunohistochemical analysis (LM *ANOVA $F$=78.804, $p$=0.000, §ANOVA $F$=66.663, $p$=0.000, MT *ANOVA $F$=7.108, $p$=0.000). (B) The mRNA levels of proinflammatory markers were detected by RT-PCR in the striatum of LRRK2 G2019S (MT) and littermate (LM) control mice (ANOVA $F$=3.602, $p$=0.052). (*$p$<0.05, between the MMP-8i and vehicle (Veh) injection groups; §$p$<0.05, between MT and LM mice). Data are expressed as the mean ± SEM of four independent experiments. Scale bars indicate 50 μm.

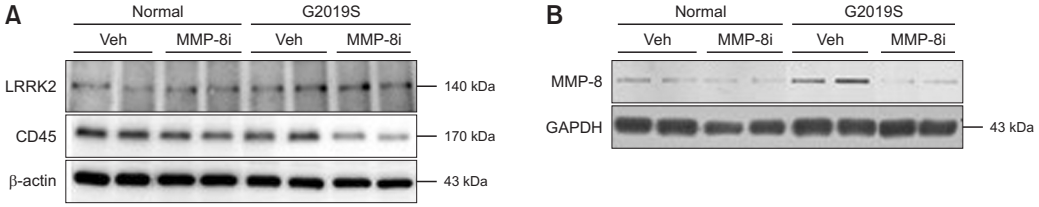


**Fig. 2.** The effects of MMP-8i on protein expression levels in the striatum of LRRK2 G2019S mice. The protein levels of LRRK2, CD45, and MMP8 were detected from the striatum sample of LRRK2 G2019S mice using Western blot (A) and slot immunoblot (B). The protein expression levels were normalized by cellular β-actin and GAPDH respectively.

ATP production in the recovery process of cellular function.

### The effect of MMP-8i on the survival of neurons in the substantia nigra and amygdala

To detect the effects of MMP-8i on neuroprotection for the survival of functional neurons in the brains of LRRK2 G2019S mice, we stained immunoreactive neurons in the substantia nigra and amygdala using immunohistochemical techniques. LRRK2 G2019S mice did not show significant differences in the number of TH-positive cells in the substantia nigra compared to normal littermate control mice (Fig. 4A). However, LRRK2 G2019S mice showed significant reduction of the cell body area of TH-positive cells in the substantia nigra compared to littermate control mice (Fig. 4A). The reduced cell body area of TH-positive cells was recovered by MMP-8i administration (Fig. 4A). LRRK2 G2019S mice showed an increased number of ChAT-positive neurons in the basolateral amygdala (BLA) region compared to littermate control mice (Fig. 4B). MMP-

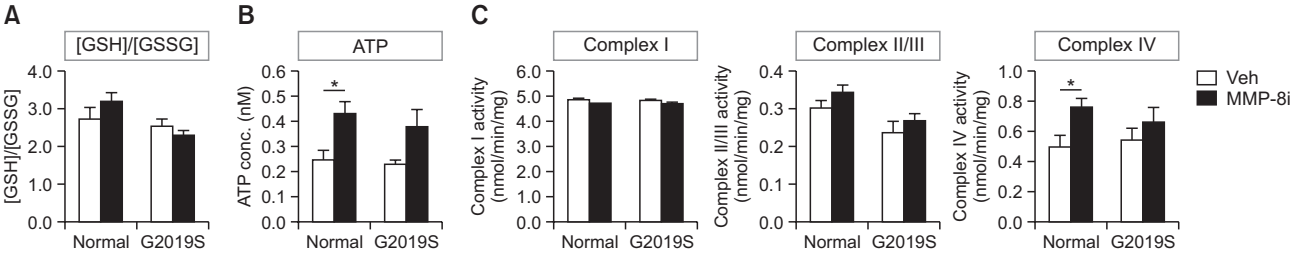


**Fig. 3.** The effects of MMP-8i on the level of GSH/GSSG, ATP, and mitochondrial complex I, II/III, and IV activities, in the striatum of LRRK2 G2019S mice. (A) Endogenous oxidative stress levels were measured by GSH/GSSG ratio that did not show significant changes by MMP-8i. (B) Oxidative phosphorylation, which was measured by ATP levels in mitochondrial fraction, showed significant increase after MMP-8i administration (ANOVA $F$=8.917, $p$=0.01). (C) Mitochondrial complex I, II/III, and IV activities were detected by substrate-enzyme reactions and complex IV activity showed significant increase by MMP-8i in littermate control mice (ANOVA $F$=6.120, $p$=0.028) (*$p$<0.05, between the MMP-8i and vehicle (Veh) injection groups). Data are expressed as the mean ± SEM of four independent experiments.

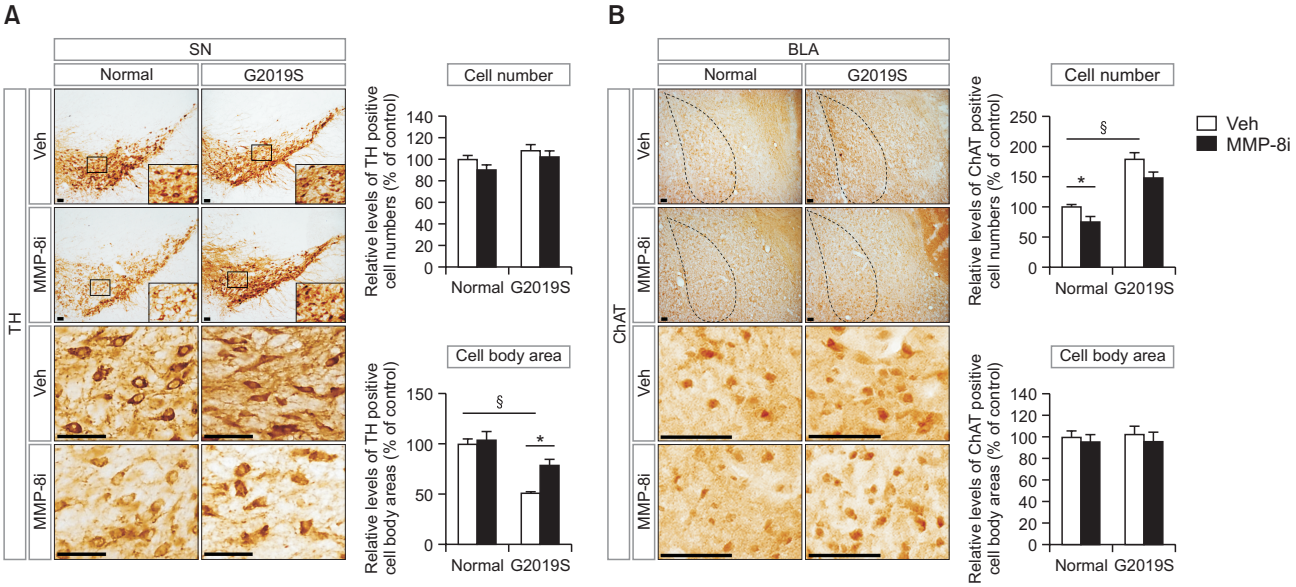


**Fig. 4.** TH-positive neurons in the substantia nigra (A) and ChAT-positive neurons in the basolateral amygdala (BLA) (B) were stained and analyzed by immunohistochemical techniques to determine the effects of MMP-8i on the population of the designated neurons (A, $^{\S}$ANOVA $F$=44.374, $p$=0.000, *ANOVA $F$=8.281, $p$=0.009; B, *ANOVA $F$=7.320, $p$=0.008, $^{\S}$ANOVA $F$=85.116, $p$=0.000) (*$p$<0.05, between the MMP-8i and vehicle (Veh) injection groups; $^{\S}p$<0.05, between MT and LM mice, n=7 for each experimental group). Data are expressed as the mean ± SEM of four independent experiments. Scale bars indicate 50 μm.

8i significantly decreased the number of ChAT-positive neurons in the BLA region of littermate control mice, but did not show significant change of the cell body area of ChAT-positive neurons in LRRK2 G2019S mice. These results suggest that MMP-8i could affect the morphology of dopaminergic neurons in the substantia nigra of LRRK2 G2019S mice and number of cholinergic neurons in the BLA region of littermate control mice.

## Behavioral improvement in LRRK2 G2019S mice after MMP-8i administration

To evaluate the effects of MMP-8i on the locomotor activities and anxiety-related behavior of experimental mice, we performed the rota-rod and open field tests. LRRK2 G2019S mice showed a significantly decreased latency to fall in the rota-rod test, indicating abnormal motor coordination that may represent PD-like motor behavior (Fig. 5A). LRRK2 G2019S mice did not show significant differences in rearing counts in the open field test (Fig. 5B), though they had a decreased amount of time spent in center area ($p$=0.057), indicating increased anxiety-like activities (Fig. 5C) (Kallai *et al.*, 2007). MMP-8i administration induced a significant increase in the latency to fall in the rota-rod test and in the time spent in the center area in the open field test when compared to the vehicle injection group (Fig. 5A, 5C). Mice that were administered MMP-8i showed no significant change in rearing counts, indicating exploratory behavior, compared to the vehicle group in LRRK2 G2019S and littermate control mice (Fig. 5B). Taken together, our results suggest that inhibition of MMP-8 improved motor balance and anxiety-like behavior in LRRK2 G2019S mice.

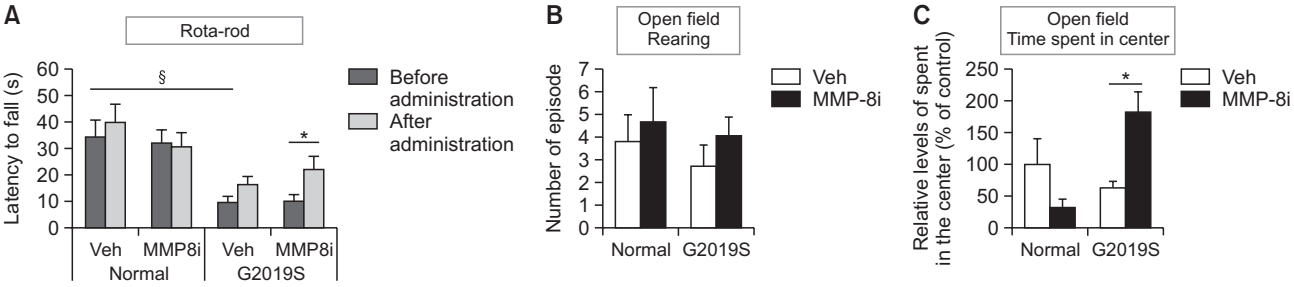


**Fig. 5.** The effect of MMP-8i on motor behavior in LRRK2 G2019S mice using the rota-rod test and the open field test. (A) Latency to fall was detected to evaluate motor coordination in the rota-rod test. (B) Rearing was counted in the open field test to detect general activity. (C) Time spent in the center was counted in the open field test to detect anxiety-like activity (ANOVA $F$=10.980, $p$=0.008) (*$p$<0.05, between the MMP-8i and vehicle (Veh) injection groups; $^{§}p$<0.05, between MT and LM mice). Data are expressed as the mean ± SEM of four independent experiments.

## DISCUSSION

In this study, we investigated the *in vivo* function of MMP-8 in LRRK2 G2019S mice by determining the effects of pharmacological inhibition of MMP-8 on proinflammatory mediators, MMP-8 expression, mitochondrial function, neuronal populations, and motor/non-motor behavior in LRRK2 G2019S PD model mice.

The number of Iba1-positive activated microglia increased in the striatum of LRRK2 G2019S mice when compared to the littermate controls and decreased after MMP-8i injection in both LRRK2 G2019S and littermate control mice (Fig. 1). We previously reported that MMP-8i suppressed microglial activation and proinflammatory cytokines in the mouse brain of sepsis and ischemic stroke (Lee *et al*., 2014; Han *et al*., 2016). These data support the anti-inflammatory effect of MMP-8i under neuroinflammatory conditions. Interestingly, MMP-8i decreased the expression level of MMP-8 in the striatum of LRRK2 G2019S mice (Fig. 2B). These results collectively indicate that MMP-8i inhibits not only the enzymatic activity but also the expression of MMP-8 in the PD mouse brain.

Oxidative stress levels as measured by GSH/GSSG did not significantly increase in LRRK2 G2019S mice compared to littermate controls, nor did MMP-8i injection produce significant differences (Fig. 3A). Increases in cellular oxidative stress levels can often cause neuronal degeneration. However, because we could not find any significant changes in endogenous oxidative stress levels as measured by GSH/GSSG, the enhancement of oxidative phosphorylation after MMP-8i injection was presumably not through tentative reduction of endogenous oxidative stress levels.

Previous studies have reported a correlation between MMPs and mitochondrial dysfunction. Reactive oxygen species induced both the expression and activity of MMP-2, resulting in a negative feedback mechanism that disrupted mitochondrial function and membrane potential (Nelson and Melendez, 2004). MMP-13 also decreased mitochondrial protein translation and ATP biosynthesis (Li *et al*., 2010a). Inhibition of MMP-2 by a pharmacological inhibitor or its siRNA prevented glucose-induced mitochondrial dysfunction in retinal endothelial cells (Mohammad and Kowluru, 2010). In the present study, we found that MMP-8i significantly increased ATP levels in the striatum of littermate control mice (but no significance was found in ATP increase in LRRK2 G2019S mice) (Fig. 3B). ATP as a product of oxidative phosphorylation in mitochondrial energetics significantly increased after treatment with MMP-8i. We presume that the increased level of ATP produces positive feedback in the progressive pathology of PD; this may result in behavioral improvement or morphological changes in neuronal architecture. Interestingly, mitochondrial complex IV activity was significantly increased by MMP-8i in littermate control mice but not in LRRK2 G2019S mice which showed very similar pattern with the increase of ATP levels by MMP-8i (Fig. 3C). These data suggest that MMP-8i can increase oxidative phosphorylation, through the enhancement of mitochondrial complex IV activity.

LRRK2 G2019S transgenic mice showed PD-like motor symptoms, including abnormal motor coordination in the rota-rod test at 20-24 months (Fig. 5), which is consistent with similar previous findings in the same transgenic mice at 12 months of age (Lin *et al*., 2009). This abnormal motor coordination of LRRK2 G2019S mice in rota-rod test was significantly improved by MMP-8i injection. LRRK2 G2019S mice did not show significant decreases in rearing in the open field test. Unlike this result, previous reports presented reduced rearing counts in LRRK2 mutant mice compared to wild type mice at 6 and 12 months of age (Li *et al*., 2010b). In contrast, we used 24 months of age for the experiment, which showed no significant differences for the rearing counts. In general, mice show decreased level of motor activities by age. So the reduced rearing counts in aged littermate normal control mice, compared to their younger age, can explain no significant differences of rearing counts in LRRK2 G2019S mice at 20-24 months of age compare to littermate control mice in this study.

Since the open field test represents not only motor function but also emotional status, we also analyzed the time spent in the center from the open field test. We found markedly decreased ($p$=0.057) time spent in center in LRRK2 G2019S mice indicating increased anxiety-like behavior (Fig. 5C), which is comparable with a previous study (Melrose *et al*., 2010). MMP-8i injection significantly increased the time spent in the center in LRRK2 G2019S mice, suggesting recovery from anxiety-like behavior, which is a typical non-motor symptom of PD patients.

The improvement of motor and non-motor symptoms of LRRK2 G2019S PD mice by MMP-8i in this study can be explained differential populations of specific neurons in the brain regions. We identified TH-positive dopaminergic neurons in the substantia nigra, and ChAT-positive cholinergic neurons in the basolateral amygdala (BLA) (Fig. 4). We could not detect

a significant decrease in TH-positive dopaminergic neurons in the substantia nigra of LRRK2 G2019S mice, which is consistent with a previous report (Li *et al*., 2010b). However, the cell body areas of TH-positive neurons were significantly decreased in the substantia nigra of LRRK2 G2019S mice compared to littermate controls. These data indicate that TH-positive neurons may undergo a progressive pathological process with abnormal morphological changes seen as decreased cell body area. Moreover, the cell body area of TH-positive cells significantly increased after MMP-8i injection, indicating improvement of cellular function and potential neuroprotection.

Anxiety-like behavior has been explained through the function of various neuronal populations, including cholinergic neurons in the basal lateral amygdala (BLA). The BLA region receives highly processed sensory information from the dorsal raphe nuclei (DRN) and sends the neuronal projections to a hypothalamic and brainstem region. LRRK2 G2019S mice showed an increased number of ChAT-positive cholinergic neurons in the BLA area, correlating with increased anxiety-like activity, which was tentatively decreased by MMP-8i (significantly in littermate controls, but not significantly in LRRK2 G2019S mutant mice). It is possible that the conditions we used in this study could not reach the required level of significance to show a decrease of the number of cholinergic neurons in the BLA region. We also did not identify any changes in cell body area after MMP-8i administration.

In conclusion, MMP-8 inhibition modulates neuroinflammation, mitochondrial function, neuronal survival, and PD-like behaviors in LRRK2 G2019S PD mice. As our previous study also suggested that MMP-8i is able to enter the brain by crossing the blood brain barrier, and exhibits anti-inflammatory and neuroprotective effects in septic mouse brains (Lee *et al*., 2014), these data collectively suggest that inhibition of MMP-8 may have therapeutic validity for various neurodegenerative diseases, including PD.

## CONFLICT OF INTEREST

The authors declare that they have no conflicts of interest.

## ACKNOWLEDGMENTS

This research was supported by NRF Grants #2017 R1A2B4008456, 2020R1H1A2013386, IITP grant from MSIT 2020-0-01343 (to HS), and #2021R1A2C1006369 (to HK).

## REFERENCES

Abdullah Thani, N. A., Sallis, B., Nuttall, R., Schubert, F. R., Ahsan, M., Davies, D., Purewal, S., Cooper, A. and Rooprai, H. K. (2012) Induction of apoptosis and reduction of MMP gene expression in the U373 cell line by polyphenolics in Aronia melanocarpa and by curcumin. *Oncol. Rep.* **28**, 1435-1442.

Balbin, M., Fueyo, A., Tester, A. M., Pendas, A. M., Pitiot, A. S., Astudillo, A., Overall, C. M., Shapiro, S. D. and Lopez-Otin, C. (2003) Loss of collagenase-2 confers increased skin tumor susceptibility to male mice. *Nat. Genet.* **35**, 252-257.

Bouhours-Nouet, N., May-Panloup, P., Coutant, R., de Casson, F. B., Descamps, P., Douay, O., Reynier, P., Ritz, P., Malthiery, Y. and Simard, G. (2005) Maternal smoking is associated with mitochondrial DNA depletion and respiratory chain complex III deficiency in placenta. *Am. J. Physiol. Endocrinol. Metab.* **288**, E171-E177.

Braak, H., Del Tredici, K., Rub, U., de Vos, R. A., Jansen Steur, E. N. and Braak, E. (2003) Staging of brain pathology related to sporadic Parkinson's disease. *Neurobiol. Aging* **24**, 197-211.

Folgueras, A. R., Fueyo, A., Garcia-Suarez, O., Cox, J., Astudillo, A., Tortorella, P., Campestre, C., Gutierrez-Fernandez, A., Fanjul-Fernandez, M., Pennington, C. J., Edwards, D. R., Overall, C. M. and Lopez-Otin, C. (2008) Collagenase-2 deficiency or inhibition impairs experimental autoimmune encephalomyelitis in mice. *J. Biol. Chem.* **283**, 9465-9474.

Frank, M. G., Baratta, M. V., Sprunger, D. B., Watkins, L. R. and Maier, S. F. (2007) Microglia serve as a neuroimmune substrate for stress-induced potentiation of CNS pro-inflammatory cytokine responses. *Brain Behav. Immun.* **21**, 47-59.

Garcia-Prieto, E., Gonzalez-Lopez, A., Cabrera, S., Astudillo, A., Gutierrez-Fernandez, A., Fanjul-Fernandez, M., Batalla-Solis, E., Puente, X. S., Fueyo, A., Lopez-Otin, C. and Albaiceta, G. M. (2010) Resistance to bleomycin-induced lung fibrosis in MMP-8 deficient mice is mediated by interleukin-10. *PLoS ONE* **5**, e13242.

Ghosh, A., Roy, A., Liu, X., Kordower, J. H., Mufson, E. J., Hartley, D. M., Ghosh, S., Mosley, R. L., Gendelman, H. E. and Pahan, K. (2007) Selective inhibition of NF-kappaB activation prevents dopaminergic neuronal loss in a mouse model of Parkinson's disease. *Proc. Natl. Acad. Sci. U.S.A.* **104**, 18754-18759.

Gueders, M. M., Balbin, M., Rocks, N., Foidart, J. M., Gosset, P., Louis, R., Shapiro, S., Lopez-Otin, C., Noel, A. and Cataldo, D. D. (2005) Matrix metalloproteinase-8 deficiency promotes granulocytic allergen-induced airway inflammation. *J. Immunol.* **175**, 2589-2597.

Gutierrez-Fernandez, A., Inada, M., Balbin, M., Fueyo, A., Pitiot, A. S., Astudillo, A., Hirose, K., Hirata, M., Shapiro, S. D., Noel, A., Werb, Z., Krane, S. M., Lopez-Otin, C. and Puente, X. S. (2007) Increased inflammation delays wound healing in mice deficient in collagenase-2 (MMP-8). *FASEB J.* **21**, 2580-2591.

Han, J. E., Lee, E. J., Moon, E., Ryu, J. H., Choi, J. W. and Kim, H. S. (2016) Matrix metalloproteinase-8 is a novel pathogenetic factor in focal cerebral ischemia. *Mol. Neurobiol.* **53**, 231-239.

Hirsch, E., Graybiel, A. M. and Agid, Y. A. (1988) Melanized dopaminergic neurons are differentially susceptible to degeneration in Parkinson's disease. *Nature* **334**, 345-348.

Hirsch, E. C., Orieux, G., Muriel, M. P., Francois, C. and Feger, J. (2003) Nondopaminergic neurons in Parkinson's disease. *Adv. Neurol.* **91**, 29-37.

Jeon, J., Kim, W., Jang, J., Isacson, O. and Seo, H. (2016) Gene therapy by proteasome activator, PA28gamma, improves motor coordination and proteasome function in Huntington's disease YAC128 mice. *Neuroscience* **324**, 20-28.

Kallai, J., Makany, T., Csatho, A., Karadi, K., Horvath, D., Kovacs-Labadi, B., Jarai, R., Nadel, L. and Jacobs, J. W. (2007) Cognitive and affective aspects of thigmotaxis strategy in humans. *Behav. Neurosci.* **121**, 21-30.

Kim, Y. S., Choi, D. H., Block, M. L., Lorenzl, S., Yang, L., Kim, Y. J., Sugama, S., Cho, B. P., Hwang, O., Browne, S. E., Kim, S. Y., Hong, J. S., Beal, M. F. and Joh, T. H. (2007) A pivotal role of matrix metalloproteinase-3 activity in dopaminergic neuronal degeneration via microglial activation. *FASEB J.* **21**, 179-187.

Kumar, H., Jo, M. J., Choi, H., Muttigi, M. S., Shon, S., Kim, B. J., Lee, S. H. and Han, I. B. (2018) Matrix metalloproteinase-8 inhibition prevents disruption of blood-spinal cord barrier and attenuates inflammation in rat model of spinal cord injury. *Mol. Neurobiol.* **55**, 2577-2590.

Lee, E. J., Han, J. E., Woo, M. S., Shin, J. A., Park, E. M., Kang, J. L., Moon, P. G., Baek, M. C., Son, W. S., Ko, Y. T., Choi, J. W. and Kim, H. S. (2014) Matrix metalloproteinase-8 plays a pivotal role in neuroinflammation by modulating TNF-alpha activation. *J. Immunol.* **193**, 2384-2393.

Lee, E. J., Park, J. S., Lee, Y. Y., Kim, D. Y., Kang, J. L. and Kim, H. S. (2018) Anti-inflammatory and anti-oxidant mechanisms of an MMP-8 inhibitor in lipoteichoic acid-stimulated rat primary astrocytes: involvement of NF-κB, Nrf2, and PPAR-γ signaling pathways. *J. Neuroinflammation* **15**, 326.

Lee, E. J., Woo, M. S., Moon, P. G., Baek, M. C., Choi, I. Y., Kim, W. K.,

Junn, E. and Kim, H. S. (2010) Alpha-synuclein activates microglia by inducing the expressions of matrix metalloproteinases and the subsequent activation of protease-activated receptor-1. *J. Immunol.* **185**, 615-623.

Leem, Y. H., Park, J. S., Park, J. E., Kim, D. Y., Kang, J. L. and Kim, H. S. (2020) Papaverine inhibits α-synuclein aggregation by modulating neuroinflammation and matrix metalloproteinase-3 expression in the subacute MPTP/P mouse model of Parkinson's disease. *Biomed. Pharmacother.* **130**, 110576.

Levin, J., Giese, A., Boetzel, K., Israel, L., Hogen, T., Nubling, G., Kretzschmar, H. and Lorenzl, S. (2009) Increased alpha-synuclein aggregation following limited cleavage by certain matrix metalloproteinases. *Exp. Neurol.* **215**, 201-208.

Li, C. H., Cheng, Y. W., Liao, P. L., Yang, Y. T. and Kang, J. J. (2010a) Chloramphenicol causes mitochondrial stress, decreases ATP biosynthesis, induces matrix metalloproteinase-13 expression, and solid-tumor cell invasion. *Toxicol. Sci.* **116**, 140-150.

Li, X., Patel, J. C., Wang, J., Avshalumov, M. V., Nicholson, C., Buxbaum, J. D., Elder, G. A., Rice, M. E. and Yue, Z. (2010b) Enhanced striatal dopamine transmission and motor performance with LRRK2 overexpression in mice is eliminated by familial Parkinson's disease mutation G2019S. *J. Neurosci.* **30**, 1788-1797.

Lin, X., Parisiadou, L., Gu, X. L., Wang, L., Shim, H., Sun, L., Xie, C., Long, C. X., Yang, W. J., Ding, J., Chen, Z. Z., Gallant, P. E., Tao-Cheng, J. H., Rudow, G., Troncoso, J. C., Liu, Z., Li, Z. and Cai, H. (2009) Leucine-rich repeat kinase 2 regulates the progression of neuropathology induced by Parkinson's-disease-related mutant alpha-synuclein. *Neuron* **64**, 807-827.

Liu, B. (2006) Modulation of microglial pro-inflammatory and neurotoxic activity for the treatment of Parkinson's disease. *AAPS J.* **8**, E606-E621.

Lorenzl, S., Albers, D. S., Narr, S., Chirichigno, J. and Beal, M. F. (2002) Expression of MMP-2, MMP-9, and MMP-1 and their endogenous counterregulators TIMP-1 and TIMP-2 in postmortem brain tissue of Parkinson's disease. *Exp. Neurol.* **178**, 13-20.

Lorenzl, S., Calingasan, N., Yang, L., Albers, D. S., Shugama, S., Gregorio, J., Krell, H. W., Chirichigno, J., Joh, T. and Beal, M. F. (2004) Matrix metalloproteinase-9 is elevated in 1-methyl-4-phenyl-1,2,3,6-tetrahydropyridine-induced parkinsonism in mice. *Neuromolecular Med.* **5**, 119-132.

Lyons, A., Downer, E. J., Crotty, S., Nolan, Y. M., Mills, K. H. and Lynch, M. A. (2007) CD200 ligand receptor interaction modulates microglial activation *in vivo* and *in vitro*: a role for IL-4. *J. Neurosci.* **27**, 8309-8313.

Melrose, H. L., Dachsel, J. C., Behrouz, B., Lincoln, S. J., Yue, M., Hinkle, K. M., Kent, C. B., Korvatska, E., Taylor, J. P., Witten, L., Liang, Y. Q., Beevers, J. E., Boules, M., Dugger, B. N., Serna, V. A., Gaukhman, A., Yu, X., Castanedes-Casey, M., Braithwaite, A. T., Ogholikhan, S., Yu, N., Bass, D., Tyndall, G., Schellenberg, G. D., Dickson, D. W., Janus, C. and Farrer, M. J. (2010) Impaired dopaminergic neurotransmission and microtubule-associated protein tau alterations in human LRRK2 transgenic mice. *Neurobiol. Dis.* **40**, 503-517.

Mohammad, G. and Kowluru, R. A. (2010) Matrix metalloproteinase-2 in the development of diabetic retinopathy and mitochondrial dysfunction. *Lab. Invest.* **90**, 1365-1372.

Moon, M., Kim, H. G., Hwang, L., Seo, J. H., Kim, S., Hwang, S., Kim, S., Lee, D., Chung, H., Oh, M. S., Lee, K. T. and Park, S. (2009) Neuroprotective effect of ghrelin in the 1-methyl-4-phenyl-1,2,3,6-tetrahydropyridine mouse model of Parkinson's disease by blocking microglial activation. *Neurotox. Res.* **15**, 332-347.

Nelson, K. K. and Melendez, J. A. (2004) Mitochondrial redox control of matrix metalloproteinases. *Free Radic. Biol. Med.* **37**, 768-784.

Orenstein, S. J., Kuo, S. H., Tasset, I., Arias, E., Koga, H., Fernandez-Carasa, I., Cortes, E., Honig, L. S., Dauer, W., Consiglio, A., Raya, A., Sulzer, D. and Cuervo, A. M. (2013) Interplay of LRRK2 with chaperone-mediated autophagy. *Nat. Neurosci.* **16**, 394-406.

Rooprai, H. K., Rucklidge, G. J., Panou, C. and Pilkington, G. J. (2000) The effects of exogenous growth factors on matrix metalloproteinase secretion by human brain tumour cells. *Br. J. Cancer* **82**, 52-55.

Ros-Bernal, F., Hunot, S., Herrero, M. T., Parnadeau, S., Corvol, J. C., Lu, L., Alvarez-Fischer, D., Carrillo-de Sauvage, M. A., Saurini, F., Coussieu, C., Kinugawa, K., Prigent, A., Hoglinger, G., Hamon, M., Tronche, F., Hirsch, E. C. and Vyas, S. (2011) Microglial glucocorticoid receptors play a pivotal role in regulating dopaminergic neurodegeneration in parkinsonism. *Proc. Natl. Acad. Sci. U.S.A.* **108**, 6632-6637.

Schubert-Unkmeir, A., Konrad, C., Slanina, H., Czapek, F., Hebling, S. and Frosch, M. (2010) Neisseria meningitidis induces brain microvascular endothelial cell detachment from the matrix and cleavage of occludin: a role for MMP-8. *PLoS Pathog.* **6**, e1000874.

Seo, H., Kim, W. and Isacson, O. (2008) Compensatory changes in the ubiquitin-proteasome system, brain-derived neurotrophic factor and mitochondrial complex II/III in YAC72 and R6/2 transgenic mice partially model Huntington's disease patients. *Hum. Mol. Genet.* **17**, 3144-3153.

Seo, H., Sonntag, K. C. and Isacson, O. (2004) Generalized brain and skin proteasome inhibition in Huntington's disease. *Ann. Neurol.* **56**, 319-328.

Smith, W. W., Pei, Z., Jiang, H., Dawson, V. L., Dawson, T. M. and Ross, C. A. (2006) Kinase activity of mutant LRRK2 mediates neuronal toxicity. *Nat. Neurosci.* **9**, 1231-1233.

Solan, P. D., Dunsmore, K. E., Denenberg, A. G., Odoms, K., Zingarelli, B. and Wong, H. R. (2012) A novel role for matrix metalloproteinase-8 in sepsis. *Crit. Care Med.* **40**, 379-387.

Sorsa, T., Tervahartiala, T., Leppilahti, J., Hernandez, M., Gamonal, J., Tuomainen, A. M., Lauhio, A., Pussinen, P. J. and Mäntylä, P. (2011) Collagenase-2 (MMP-8) as a point-of-care biomarker in periodontitis and cardiovascular diseases. Therapeutic response to non-antimicrobial properties of tetracyclines. *Pharmacol. Res.* **63**, 108-113.

Sung, J. Y., Park, S. M., Lee, C. H., Um, J. W., Lee, H. J., Kim, J., Oh, Y. J., Lee, S. T., Paik, S. R. and Chung, K. C. (2005) Proteolytic cleavage of extracellular secreted {alpha}-synuclein via matrix metalloproteinases. *J. Biol. Chem.* **280**, 25216-25224.

van der Zijl, N. J., Hanemaaijer, R., Tushuizen, M. E., Schindhelm, R. K., Boerop, J., Rustemeijer, C., Bilo, H. J., Verheijen, J. H. and Diamant, M. (2010) Urinary matrix metalloproteinase-8 and -9 activities in type 2 diabetic subjects: a marker of incipient diabetic nephropathy? *Clin. Biochem.* **43**, 635-639.

Van Lint, P., Wielockx, B., Puimège, L., Noël, A., López-Otin, C. and Libert, C. (2005) Resistance of collagenase-2 (matrix metalloproteinase-8)-deficient mice to TNF-induced lethal hepatitis. *J. Immunol.* **175**, 7642-7649.

Väyrynen, J. P., Vornanen, J., Tervahartiala, T., Sorsa, T., Bloigu, R., Salo, T., Tuomisto, A. and Mäkinen, M. J. (2012) Serum MMP-8 levels increase in colorectal cancer and correlate with disease course and inflammatory properties of primary tumors. *Int. J. Cancer* **131**, E463-E474.

Zitka, O., Skalickova, S., Gumulec, J., Masarik, M., Adam, V., Hubalek, J., Trnkova, L., Kruseova, J., Eckschlager, T. and Kizek, R. (2012) Redox status expressed as GSH:GSSG ratio as a marker for oxidative stress in paediatric tumour patients. *Oncol. Lett.* **4**, 1247-1253.